Supplementary Figure Legends

Figure S1. Confirmation of functionality of the Chk1 inhibitors in Raji. Functionality of the Chk1 inhibitors UCN-01 and TCS2312 in the applied concentrations was assessed by Immunoblot analysis of CDC25A accumulation.

Figure S2. Evidence of more than two Chk1 alleles by Southern blot. Southern blot analysis of DT40Cre1 wild type cells and independent subclones with one, two or three Chk1 alleles deleted. BamHI-digested genomic DNA was hybridized with the 3' probe shown in Fig. 2a. The probe hybridizes to a 6.0 and 4.6 kb genomic fragment, derived from the wild-type and Chk1-targeted alleles, respectively.

Figure S3. Principle of the measurement of Ig diversification in DT40ΨV$^-$ and DT40Cre1 (Arakawa et al. 2004). (a) Measurement of somatic hypermutation in DT40ΨV$^-$. The pseudogenes of the rearranged light chain locus required for Ig gene conversion were deleted, leading to a block in Ig gene conversion and an increase in somatic hypermutation at dG/dC. Somatic hypermutation can be measured by an IgM loss assay, in which IgM-positive cells are subcloned and analyzed for the formation of IgM-negative cells arising due to hypermutation-derived deleterious mutations (b) Measurement of Ig gene conversion and somatic hypermutation in DT40Cre1. The DT40Cre1 cell line still contains its pseudogenes and Ig diversification is based mainly on Ig gene conversion and only to a very minor part on somatic hypermutation. Moreover, the DT40Cre1 cell line contains a frameshift mutation in its rearranged light chain locus and is therefore predominantly IgM negative. Ig gene conversion can be measured by an IgM reversion assay, in which IgM-negative cells are subcloned and analyzed for the formation of IgM-positive cells, which arise due to replacement of the frameshift mutation by templated Ig gene conversion events.

Figure S4. Confirmation of Chk1 depletion in DT40 Cre1. (a) Southern blot analysis of DT40Cre1 wild type as well as of two independent subclones of the indicated genotype. BamHI-digested genomic DNA was hybridized with the 3' probe shown in Fig. 2a. The probe hybridizes to a 6.0 and 4.6 kb genomic fragment derived from the wild-type and Chk1-targeted alleles. (b) Immunoblot analysis of Chk1 and AID expression of the clones analyzed in (a). Two different exposures are shown for Chk1.

Figure S5. Mutation distributions in the VJλ-region in representative subclones of DT40Cre1 and Chk1 targeted derivatives. Each horizontal line is a map of mutational events in one individual clone of the indicated genotype. The number next to the horizontal line indicates the number of identical sequences detected. Nucleotide positions and the location of the three CDRs are given in the line at the top. The numbering of the base pairs starts with the beginning of the leader exon. The arrow indicates the location of the frameshift mutation of the DT40Cre1 cell line. Filled circles represent non-templated point mutations and white circles ambiguous mutations that could neither be ascribed to a non-templated mutation nor a templated Ig gene conversion event. Grey rectangles represent the maximum length and black rectangles the minimum length of an Ig gene conversion event. Next to each gene conversion event, the most likely pseudogene donor (Ψ) with which recombination occurred is indicated. In case of overlap of potential Ig gene conversion tract length, the second event is indicated below the respective line.

Table S1. Chk1 targeting efficiencies in DT40ΨV$^-$

Chk1 genotype before transfection	No. of drug-resistant clones	No. of PCR-positive clones	Targeting efficiency (%)
+/+/+/+	67	19	28.4
+/+/+/-	48	15	31.3
+/+/-/-	248	3	1.2 ***

[a] *** = p < 0.001; Fisher's Exact Test

Table S2. Sequencing of Bcl6 in wildtype and Chk1+/+/-/- DT40ΨV$^-$ cells

Chk1 genotype	No. of sequences	total bp sequenced	Mutation events	Mutations / basepair (x10^{-4})
+/+/+/+	40	25200	3	1,19
+/+/-/-	30	18900	0	0

Table S3. Targeted integration efficiencies in wild-type, Chk1+/+/+/- und Chk1+/+/-/- DT40 cells

	Rad18			RDM1		
Chk1 genotype	No. of drug-resistant clones	No. of PCR-positive clones	Targeting efficiency (%)	No. of drug-resistant clones	No. of PCR-positive clones	Targeting efficiency (%)
+/+/+/+	82	16	19.5	69	45	65.2
+/+/+/-	73	17	23.3	72	46	63.9
+/+/-/-	111	23	20.7	121	59	48.8* [a]

[a] * = p = 0.03; Fisher's Exact Test

Table S4. Primers binding in the respective resistance cassette used for targeted integration screening

Resistance cassette	Primer sequence
Puromycin	5'-CAG CGC CCG ACC GAA AGG AGC GCA-3'
Blasticidin	5'-CGA TTG AAG AAC TCA TTC CAC TCA AAT-3'
Gpt	5'-TCGTATTCGTCCCGCCAATCTCCGGTCGCT-3'
Bleomycine	5'-GTC GTG TCC ACG AAC TTC C-3'

Figure S1

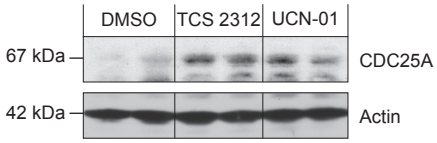

Figure S2

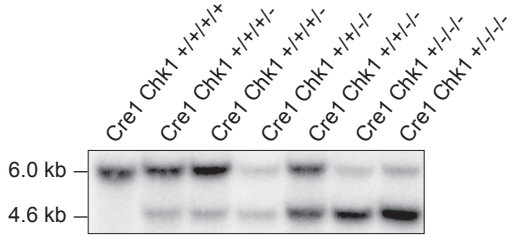
Cre1 Chk1 +/+/+/+
Cre1 Chk1 +/+/+/-
Cre1 Chk1 +/+/+/-
Cre1 Chk1 +/+/-/-
Cre1 Chk1 +/+/-/-
Cre1 Chk1 +/-/-/-
Cre1 Chk1 +/-/-/-
6.0 kb
4.6 kb

Figure S3

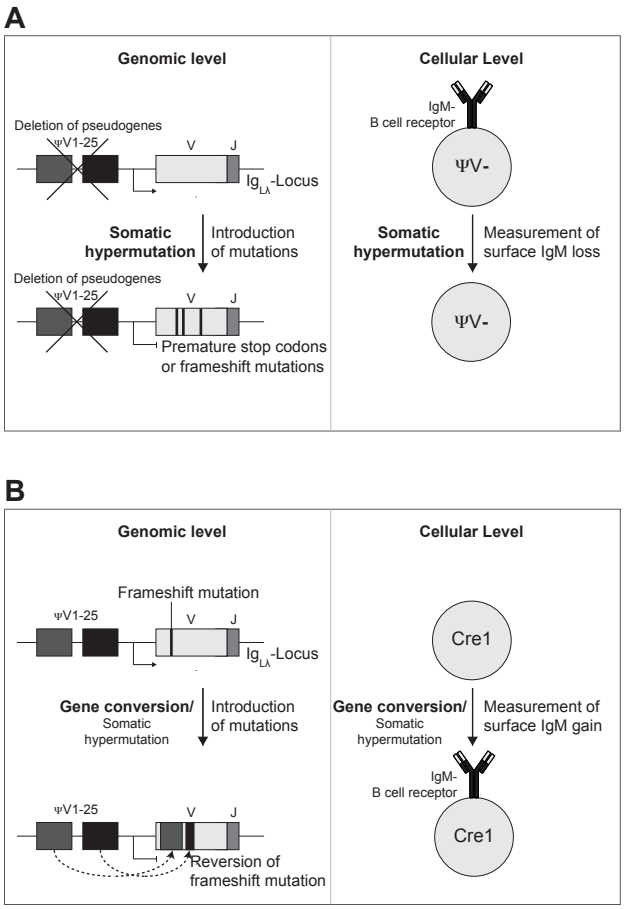
A
Genomic level
Cellular Level
Deletion of pseudogenes
ΨV1-25
V
J
Ig$_{LA}$-Locus
IgM-
B cell receptor
ΨV-
Somatic
hypermutation
Introduction
of mutations
Measurement of
surface IgM loss
Deletion of pseudogenes
ΨV1-25
V
J
Premature stop codons
or frameshift mutations
ΨV-
B
Genomic level
Cellular Level
Frameshift mutation
ΨV1-25
V
J
Ig$_{LA}$-Locus
Cre1
Gene conversion/
Somatic
hypermutation
Introduction
of mutations
Gene conversion/
Somatic
hypermutation
Measurement of
surface IgM gain
IgM-
B cell receptor
ΨV1-25
V
J
Reversion of
frameshift mutation
Cre1

Figure S4

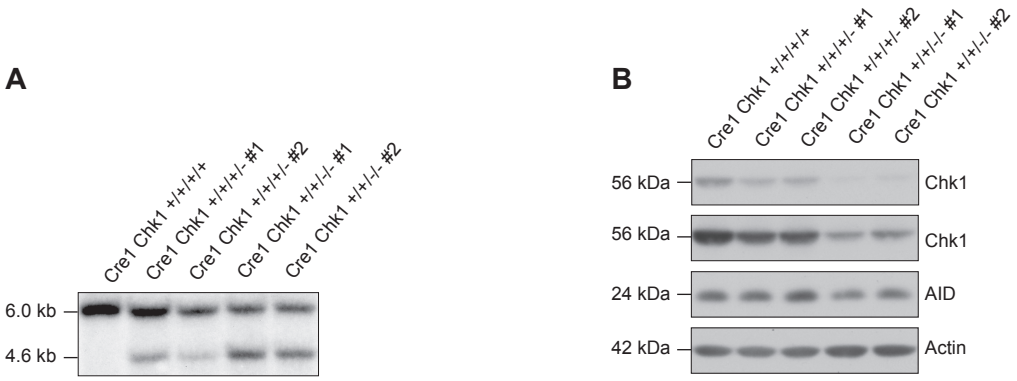
A
Cre1 Chk1 +/+/+/+
Cre1 Chk1 +/+/+/- #1
Cre1 Chk1 +/+/+/- #2
Cre1 Chk1 +/+/-/- #1
Cre1 Chk1 +/+/-/- #2
6.0 kb
4.6 kb
B
Cre1 Chk1 +/+/+/+
Cre1 Chk1 +/+/+/- #1
Cre1 Chk1 +/+/+/- #2
Cre1 Chk1 +/+/-/- #1
Cre1 Chk1 +/+/-/- #2
56 kDa
Chk1
56 kDa
Chk1
24 kDa
AID
42 kDa
Actin

Figure S5

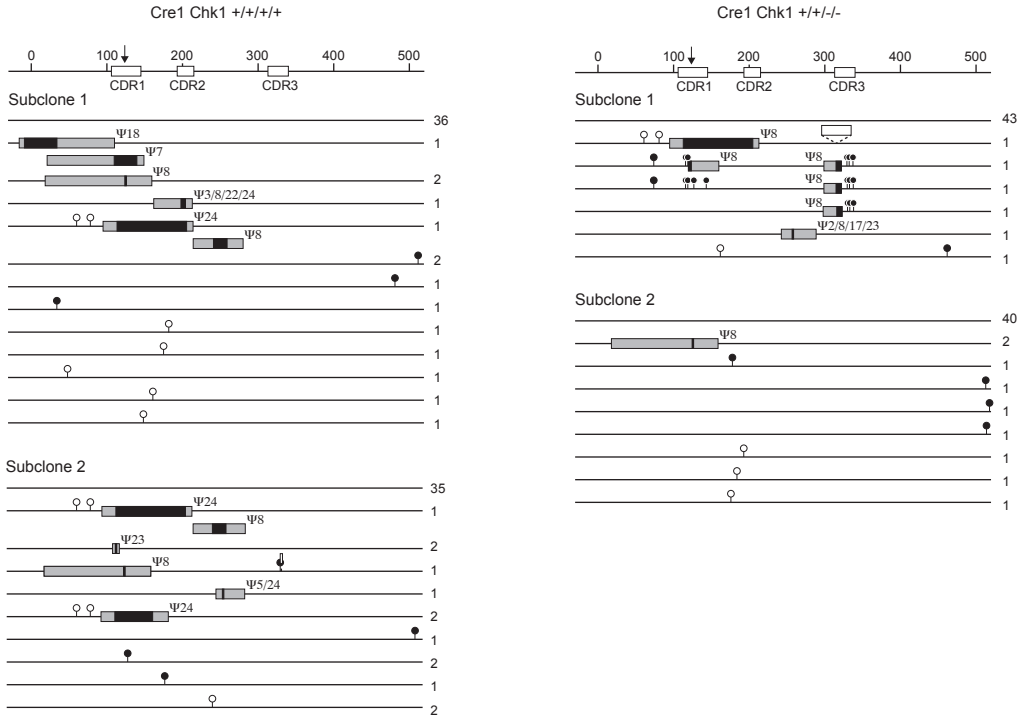
Cre1 Chk1 +/+/+/+
0
100
200
300
400
500
CDR1
CDR2
CDR3
Subclone 1
Ψ18
Ψ7
Ψ8
Ψ3/8/22/24
Ψ24
Ψ8
36
1
2
1
1
2
1
1
1
1
1
1
1
Subclone 2
Ψ24
Ψ8
Ψ23
Ψ8
Ψ5/24
Ψ24
35
1
2
1
1
2
1
2
1
2
Cre1 Chk1 +/+/-/-
0
100
200
300
400
500
CDR1
CDR2
CDR3
Subclone 1
Ψ8
Ψ8
Ψ8
Ψ8
Ψ8
Ψ2/8/17/23
43
1
1
1
1
1
1
Subclone 2
Ψ8
40
2
1
1
1
1
1
1
1